OXFORD

SOT | Society of Toxicology
www.toxsci.oxfordjournals.org

TOXICOLOGICAL SCIENCES, 153(1), 2016, 89–102

doi: 10.1093/toxsci/kfw105
Advance Access Publication Date: June 2, 2016
Research article

Characterization of Hepatotoxicity Mechanisms Triggered by Designer Cathinone Drugs (β-Keto Amphetamines)

Maria João Valente,* Ana Margarida Araújo,* Maria de Lourdes Bastos,* Eduarda Fernandes,† Félix Carvalho,* Paula Guedes de Pinho,* and Márcia Carvalho*,‡,[1]

*UCIBIO, REQUIMTE, Laboratory of Toxicology, Faculty of Pharmacy, University of Porto, Porto, Portugal; †UCIBIO, REQUIMTE, Laboratory of Applied Chemistry, Faculty of Pharmacy, University of Porto, Porto, Portugal; and ‡FP-ENAS, CEBIMED, Fundação Ensino e Cultura Fernando Pessoa, Porto, Portugal

[1]To whom correspondence should be addressed at FP-ENAS, CEBIMED, Fundação Ensino e Cultura Fernando Pessoa, Praûïa 9 de Abril, 349, 4249-004 Porto, Portugal. Fax: +351 225074630. E-mail address: mcarv@ufp.edu.pt.

ABSTRACT

The use of cathinone designer drugs in recreational settings has been associated with severe toxic effects, including liver damage. The precise mechanisms by which cathinones induce hepatotoxicity and whether they act by common pathways remain to be elucidated. Herein, we assessed the toxicity of the cathinones methylone, pentedrone, 3,4-methylenedioxypyrovalerone (MDPV) and 4-methylethcathinone (4-MEC) in primary rat hepatocytes (PRH) and HepaRG cells, and compared with that of 3,4-methylenedioxymethamphetamine (MDMA). MDPV and pentedrone were significantly more toxic than MDMA, while methylone was the least cytotoxic compound. Importantly, PRH revealed to be the most sensitive experimental model and was thus used to explore the mechanisms underlying the observed toxicity. All drugs elicited the formation of reactive oxygen and nitrogen species (ROS and RNS), but more markedly for methylone, pentedrone and 4-MEC. GSH depletion was also a common effect at the highest concentration tested, whereas only MDPV and pentedrone caused a significant decrease in ATP levels. The antioxidants ascorbic acid or *N*-acetyl-L-cysteine partially attenuated the observed cell death. All cathinones triggered significant caspase activation and apoptosis, which was partially reversed by the caspase inhibitor Ac-LETD-CHO. In conclusion, the present data shows that (1) cathinones induce *in vitro* hepatotoxic effects that vary in magnitude among the different analogues, (2) oxidative stress and mitochondrial dysfunction play a role in cathinones-induced hepatic injury, and (3) apoptosis appears to be an important pathway of cell death elicited by these novel drugs.

Key words: synthetic cathinones; β-keto amphetamines; hepatotoxicity; oxidative stress; apoptosis.

In the past few decades, classical illicit drugs have been gradually losing ground to new psychoactive substances (NPS), especially among young adult users in recreational settings (Burns *et al.*, 2014; Helander *et al.*, 2014; Maxwell, 2014). Synthetic cathinones, often deceivingly labelled as 'bath salts', are a major family of NPS that encompasses a large number of psychoactive substances deliberately designed to mimic the effects of controlled drugs of abuse (Karila *et al.*, 2015). According to the European Monitoring Centre for Drugs and Drug Addiction (EMCDDA), synthetic cathinones were the largest category of NPS identified in Europe in 2014, with 31 new derivatives reported for the first time that year (EMCDDA, 2015a). 3,4-Methylenedioxymethcathinone (methylone), 3,4-methylenedioxypyrovalerone (MDPV), α-methylaminovalerophenone (pentedrone) and 4-methylethcathinone (4-MEC) are four of the most commonly used derivatives worldwide (Elliott and Evans,

2014; Moran and Seely, 2014). Together, these four derivatives covered over 40% of all samples of synthetic cathinones seized in Europe in 2013 (EMCDDA, 2015b), and were in the top five of most consumed synthetic cathinones in the United States in the same year (DEA, U.S 2014). Along with the paradigm shift in recreational drug use, several reports of intoxication and deaths related to the use of designer cathinone drugs have been described in Maskell *et al.* (2011), Regunath *et al.* (2012), Ross *et al.* (2011), and in particular with these 4 derivatives (Gil *et al.*, 2013; Murray *et al.*, 2012; Pearson *et al.*, 2012; Sykutera *et al.*, 2015), raising a global health concern over the abuse of these NPS.

Chemically, synthetic cathinones are related to amphetamines, bearing a ketone group at the β-position of the side chain, and are therefore often named β-keto amphetamines (Prosser and Nelson, 2012). Functional group substitutions to the core structure of the parent cathinone compound have yielded a large number of NPS on the street and cyber drug markets (EMCDDA, 2015b), which can be separated into different chemical families based on the substitutions made (Valente *et al.*, 2014). The most basic derivatives are the *N*-alkylated derivatives, which may present alkyl substitutions in the α-carbon of the side chain and in the benzyl ring. When a 3,4-methylenedioxy group is added to the benzyl ring, cathinones structurally similar to 3,4-methylenedioxyamphetamines are produced (Kelly, 2011). The pyrrolidinophenone-like family encompasses derivatives containing a pyrrolidine substitution in the nitrogen atom (Westphal *et al.*, 2007), which can be further modified to combine the pyrrolidine moiety and a 3,4-methylenedioxy ring (Kelly, 2011), yielding more complex cathinones. Importantly, the apparent boom in NPS creates a new challenge from a chemical and biological point of view, as structures, solubility and redox potential of the designer drugs differ between NPS and the prototype drugs they are derived from (den Hollander *et al.*, 2014). Generally, the presence of the β-keto group increases the polarity of cathinone derivatives, resulting in a decrease of their ability to cross lipid bilayer membranes, such as the blood-brain barrier (BBB) (Simmler *et al.*, 2013, 2014), which consequently decreases the potency of synthetic cathinones when compared with their related amphetamines. For this reason, users often resort to higher doses or binge consumption of cathinone derivatives to attain equipotent effects (Prosser and Nelson, 2012). The polarity issue occurs mainly with the *N*-alkylated derivatives, but not so much with the pyrrolidine family of cathinones, since the presence of the pyrrolidine ring greatly reduces the polarity of these compounds (Coppola and Mondola, 2012), resulting in a greater transport of derivatives such as MDPV through the BBB.

Designer cathinone drugs exert their stimulant effects by interacting with monoamine membrane transporters, namely dopamine (DA), norepinephrine (NE), and serotonin (5-HT) transporters (Baumann *et al.*, 2012; Cozzi *et al.*, 1999; Eshleman *et al.*, 2013; Kelly, 2011; Lopez-Arnau *et al.*, 2012). However, considerable differences have been found in the affinities towards these transporters among the different substituted cathinones *in vitro*. Methylone, like amphetamines (Sitte and Freissmuth, 2010), acts as a substrate for monoamine transporters to induce reverse transport of neurotransmitters, which consequently leads to increased concentration of these biogenic amines in the synaptic cleft, but with weaker potency than MDMA (Baumann *et al.*, 2012). Conversely, MDPV and pentedrone function as pure transporter blockers, resembling cocaine, inhibiting the uptake of DA and NE, with minimal effects on 5-HT uptake (Baumann *et al.*, 2013; Simmler, *et al.*, 2014). 4-MEC presents a mixed mode of interaction, with a potency of inhibition similar to cocaine, but also a 5-HT release comparable to MDMA (Simmler, *et al.*, 2014). As a more dopaminergic and noradrenergic drug, MDPV induces MDMA- and cocaine-like subjective effects, including increased energy, but limited euphoria and only mild empathogenic effects (Deluca *et al.*, 2009), while methylone, 4-MEC and pentedrone users report more MDMA-like stimulating effects, such as euphoria, openness and increased sociability and sexual drive (Van Hout, 2014; www.drugs-forum.com). Whereas variations on the mode of action of synthetic cathinones appear to be determined by their chemical structure (Simmler, *et al.*, 2014), it remains to be studied whether the mechanisms of toxicity elicited by this group of NPS are also reliant on their structure. Common symptoms of 'bath-salts'-induced intoxications are consistent with sympathetic stimulation, including hypertension, hyperthermia, tachycardia and seizures, and often result in end-organ effects and death (Coppola and Mondola, 2012; Prosser and Nelson, 2012). Since ingestion is one of the preferable routes of administration for this group of NPS (Valente *et al.*, 2014), the first-pass effect renders the liver more susceptible to toxic injury, as ascertained by clinical evidences of cathinones-induced hepatic dysfunction (Borek and Holstege, 2012; Carbone *et al.*, 2013; Fröhlich *et al.*, 2011; Murray, *et al.*, 2012; Pearson, *et al.*, 2012) and organ accumulation (Marinetti and Antonides, 2013; Sykutera, *et al.*, 2015). Therefore, the aim of this study was to investigate *in vitro* the effects and mechanisms underlying the hepatotoxicity of four designer cathinone drugs belonging to different chemical families. The structures and some physicochemical properties, namely the partition coefficient (log *P*) and the acid dissociation constant (pK_a), of cathinones herein studied are presented in Table 1. Methylone, which belongs to the group containing a 3,4-methylenedioxy ring, only differs from MDMA by the presence of the β-keto group, thus earning the common designation of βk-MDMA. MDPV, from the 3,4-methylenedioxy-*N*-pyrrolidine family, is characterized by a side chain alkylation (butylation), which is also found in pentedrone. Pentedrone is included in the *N*-alkylated family, with a *N*-methyl group, as well as 4-MEC, which presents a methyl group in the benzyl ring, and a *N*-ethyl group. Considering the structural similarity of cathinone derivatives and MDMA, a comparative study was conducted. The specific objectives of this study were to (1) evaluate the cytotoxic potential of selected cathinones in primary rat hepatocytes (PRH) and HepaRG cells, and compare it to MDMA, (2) provide further chemical characterization by assessing the redox potential of cathinone derivatives, (3) elucidate the cellular mechanisms underlying the observed hepatotoxicity, specifically the induction of oxidative stress and the interference with mitochondrial function, and (4) characterize the cell death pathways involved in liver damage elicited by these NPS.

MATERIALS AND METHODS

Chemicals

Collagenase from *Clostridium histolyticum* Type IA, Williams' E medium, dexamethasone, gentamicin, insulin solution from bovine pancreas (10 mg/ml), hydrocortisone 21-hemisuccinate sodium salt, thiazolyl blue tetrazolium bromide (MTT), sodium pyruvate, β-nicotinamide adenine dinucleotide reduced disodium salt hydrate (β-NADH), L-glutathione reduced (GSH) and L-glutathione oxidized disodium salt (GSSG), β-nicotinamide adenine dinucleotide 2′-phosphate reduced tetrasodium salt hydrate (β-NADPH), 5,5′-dithiobis(2-nitrobenzoic acid) (DTNB), 2′,7′-dichlorodihydrofluorescein (DCFH) and 2′,7′-dichlorodihydrofluorescein diacetate (DCFH-DA), adenosine triphosphate (ATP), luciferase from *Photinus*

TABLE 1. Chemical Structures and Logarithmic Values of the Acid Dissociation Constant (pK_a) and the Partition Coefficient (log *P*) of the Studied Compounds

Common Name	Chemical Structures	pK_a*	Log *P**
MDMA (3,4-methylenedioxymethamphetamine)	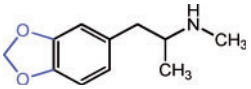	10.14	1.92
Methylone (3,4-methylenedioxy-*N*-methylcathinone)	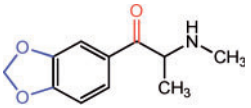	7.96	1.08
MDPV (3,4-MDPV)	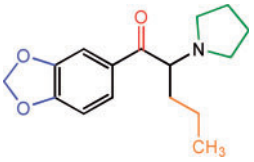	7.31	2.63
Pentedrone (α-methylaminovalerophenone)		8.20	2.26
4-MEC (4-methylethcathinone)	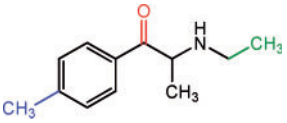	8.13	2.21

*pKa and log *P* values were calculated using MarvinSketch v.16.2.29.0 software (ChemAxon, Budapest, Hungary).

pyralis (firefly) and D-luciferin sodium salt, *N*-acetyl-Asp-Glu-Val-Asp-*p*-acetyl-Ile-Glu-Thr-Asp-*p*-nitroanilide (Ac-IETD-pNA), and *N*-acetyl-Leu-Glu-His-Asp-*p*-nitroanilide (Ac-LEHD-pNA), *N*-acetyl-Leu-Glu-Thr-Asp-aldehyde (Ac-LETD-CHO), *N*-acetyl-L-cysteine (NAC), ascorbic acid (AA) and bovine serum albumin were purchased from Sigma Aldrich (St Louis, Missouri). Heat-inactivated fetal bovine serum (FBS), antibiotic mixture of penicillin/streptomycin (10,000 U/ml/10,000 μg/ml), fungizone (250 μg/ml), and Hank's balanced salt solution (HBSS) were obtained from GIBCO Invitrogen (Barcelona, Spain). All other chemicals of analytical grade were purchased from Merck (Darmstadt, Germany). Hydrochloride salts of methylone, MDPV, pentedrone and 4-MEC were purchased online from the Sensearomatic website (http://sensearomatic.net, currently unavailable), during March 2013. MDMA was extracted, purified, and converted to the respective hydrochloride salt at UCIBIO-REQUIMTE, Laboratory of Toxicology, Faculty of Pharmacy, Porto, Portugal, from high purity MDMA tablets provided by the Portuguese Criminal Police Department. The salts were fully characterized by mass spectrometry, NMR and elemental analysis (data not shown), and purity was >98%.

In Vitro *Hepatotoxicity Cellular Models*

HepaRG cell culture. HepaRG cell line was supplied by Life Technologies Europe BV (Bleiswijk, the Netherlands) and routinely maintained in complete Williams' E medium, supplemented with 10% FBS, 100 U/ml/100 μg/ml penicillin/streptomycin, 5 μg/ml insulin and 50 μM hydrocortisone 21-hemisuccinate, and incubated at 37°C, with 5% CO_2. Cells were subcultured over 6 passages (passages 9–14). When reaching confluence, 2% DMSO was added to the culture medium to allow cell differentiation hepatocyte-like cells into adult hepatocytes and biliary epithelial cells. After a 2-week differentiation period, cells were seeded in 96-well plates at high density (0.45×10^6 cells/cm^2), and incubated overnight at 37°C, with 5% CO_2, to allow cell adhesion.

Isolation and primary culture of rat hepatocytes. Male Wistar Han rats weighing 210–250 g were purchased from Charles-River Laboratories (Barcelona, Spain). Surgical procedures were conducted under isoflurane-induced anesthesia in an isolated system, and carried out between 10.00 and 11.00 am. All experiments were approved by the Ethics Committee of the Faculty of Pharmacy, University of Porto.

Isolated rat hepatocytes were obtained through a collagenase perfusion, as previously described in Valente *et al.* (forthcoming). Cell viability was assessed through the trypan blue exclusion test and was always higher than 80%. A suspension of 0.5×10^6 viable cells/ml was cultured in 6- or 96-well plates at approximately 0.1×10^6 cells/cm^2, in Williams' E medium, supplemented with 10% FBS, 100 U/ml penicillin, 100 μg/ml streptomycin, 5 μg/ml insulin, 50 μM dexamethasone, 100 μg/ml gentamicin, and 2.5 μg/ml fungizone, and incubated overnight at 37°C, with 5% CO_2, to allow cell adhesion.

Drug Treatments

Primary cultured hepatocytes and HepaRG cells were exposed for 24 h to the four cathinones — methylone, MDPV, pentedrone and 4-MEC — and MDMA, at a wide concentration range, from 0.05 to 10 or 20 mM, in order to obtain a complete concentration-response curve in the MTT reduction assay. All incubations with the test drugs were performed in serum-free medium. For further assays, performed only in PRH, the five compounds were tested at a narrower range that includes low-effect to worst-case approach concentrations (0.2–1.6 mM). To

evaluate the effect of cytochrome P450 2D6 isoenzyme (CYP2D6) inhibitor quinidine, the antioxidants AA and NAC, or the caspases inhibitor Ac-LETD-CHO, a pre-incubation of 1 h was performed, followed by a co-incubation with MDMA or the synthetic cathinones at 1.6 mM.

Characterization of the Reducing Properties of Synthetic Cathinones

The reducing power of cathinone derivatives and MDMA was determined as described by Berker *et al.* (2007). Briefly, various concentrations (0.05–50 mM) of each compound were mixed with 0.2 M sodium phosphate buffer (pH 6.6) and 1% potassium ferricyanide (w/v). The mixture was incubated at 50°C for 20 min. After incubation, 10% tricloroacetic acid (w/v) was added and the mixture was centrifuged for 8 min at 1000 rpm, at 4°C. The upper layer was mixed with equal volume of deionised water and 0.1% of ferric chloride (w/v). Depending on the reducing potential of each compound, the yellow color of the initial solution changes to various shades of green due to the formation of Prussian blue, $KFe[Fe(CN)_6]$, from the reduction of the Fe^{3+}/ferricyanide complex to the ferrous form. Therefore, the formation of Prussian blue at 700 nm provides a measurement of the Fe^{2+} concentration in each solution. Results were obtained from three independent experiments, run in duplicate.

Cell Viability Assessment

MTT reduction and LDH leakage assays were performed as previously described (Valente *et al.*, forthcoming). Data were obtained from at least five independent experiments, performed in triplicate, and normalized to no treatment and 1% Triton X-100 controls.

Characterization of Hepatotoxicity Mechanisms Triggered by Cathinone Derivatives

Intracellular ROS and RNS formation. Intracellular production of reactive oxygen (ROS) and nitrogen (RNS) species was evaluated by the inclusion of the probe DCFH-DA (Valente *et al.*, forthcoming). As determined by incubation of MDMA or cathinone derivatives for 24 h with DCFH, in the absence of cells, no interference with the probe was noted at any tested concentration (data not shown). Results were obtained from six independent experiments, performed in triplicate, and normalized to cells with no treatment.

Intracellular GSH and GSSG levels. Total and oxidized glutathione (GSSG) intracellular contents were determined by the DTNB-GSSG reductase recycling assay (Valente *et al.*, forthcoming). GSH concentrations were calculated as follows: [GSH] = [total glutathione] – 2*[GSSG]. GSH and GSSG levels were normalized to total protein contents, as determined through the Lowry method. Results were obtained from at least four independent experiments, run in duplicate.

Intracellular ATP levels. Intracellular levels of ATP were quantified through a bioluminescence assay based on the emission of light from the reaction of ATP and luciferin, catalyzed by the enzyme luciferase (Valente *et al.*, forthcoming). No interference with the probe was noted at any tested concentration, as determined by measurement of the bioluminescence of MDMA or cathinone derivatives solutions with luciferin-luciferase assay solution in the absence of cells (data not shown). Results were obtained from at least four independent experiments, run in duplicate. ATP contents were normalized to total protein.

Characterization of Cell Death Pathways Triggered by Synthetic Cathinones

Caspase 3, 8, and 9 activity. The activity of caspases 3, 8, and 9 was determined in the cytoplasmatic fractions of primary cultured hepatocytes after a 24 h exposure to MDMA or the cathinone derivatives, as previously described (Valente *et al.*, forthcoming). Results were obtained from five independent experiments, run in duplicate. Protein contents on the cell lysate were measured using the Bio-Rad RC DC protein assay kit (Hercules, CA, USA), with albumin as the standard.

Hoechst 33342/propidium iodide fluorescent staining. Hepatocytes undergoing apoptosis or necrosis were identified based on nuclear morphological changes, using a cell-permeant nuclear counterstain that emits blue fluorescence when bound to DNA, Hoechst 33342, and a membrane impermeant nuclear dye that emits red fluorescence only in dead cells, PI (Valente *et al.*, forthcoming).

Statistical Analysis

Curves of normalized mortality values as a function of concentration, obtained through the MTT reduction assay, were constructed and analyzed as described by Dias da Silva *et al.* (2014), with a modified logit function applied as follows: $Y = \theta_{max}/(1 + \exp(-\theta_1 - \theta_2 \times \log(x)))$, where θ_{max} is the maximal observed effect, x is the concentration of the test drug, θ_1 is the parameter for the location, and θ_2 is the slope parameter. Statistical uncertainties are expressed as 95% confidence intervals (CI). Additionally, comparisons between curves (θ_{max}, θ_1 and θ_2) were performed using the extra sum-of-squares *F*-test. For further assays, results are presented as mean ± standard error of the mean (SEM). Normality of the data distribution was assessed by the D'Agostino and Pearson omnibus normality test. Multiple comparisons within each compound (concentration as a variable) or between each synthetic cathinone and MDMA were performed through one-way ANOVA analysis, followed by Fisher's LSD *posthoc* test. Non-linear curve fitting and all statistical calculations were performed using GraphPad Prism 6 (version 6.01) for Windows. *P*-values lower than .05 were considered statistically significant.

RESULTS

PRH Is a More Suitable In Vitro *Model than HepaRG to Study the Hepatotoxicity Elicited by Synthetic Cathinones*

The hepatotoxic potential of methylone, MDPV, pentedrone and 4-MEC was assessed in PRH and HepaRG cells through the MTT reduction assay. Figure 1 presents the concentration–response curves for each drug in the two used *in vitro* models. A summary of the calculated half maximal effective concentrations (EC50) of each compound, and other parameters from the nonlinear regression fit are provided in Supplementary Table S1. HepaRG cells proved to be significantly more resistant to the toxicity elicited by all five drugs, with curve fits substantially shifted to the right of PRH ones ($P < .0001$). For all four cathinones, but not MDMA, HepaRG cells presented steeper curves, with significantly higher slopes ($P < .01$ vs. PRH, when curves were compared for θ_2), which is representative of a higher variation of mortality within smaller concentration ranges in this *in vitro* model.

In order to determine whether the discrepant results between the two hepatic cellular models were due to differences in their intrinsic metabolic capacities, an additional study was conducted in the presence of quinidine, a CYP2D6 inhibitor.

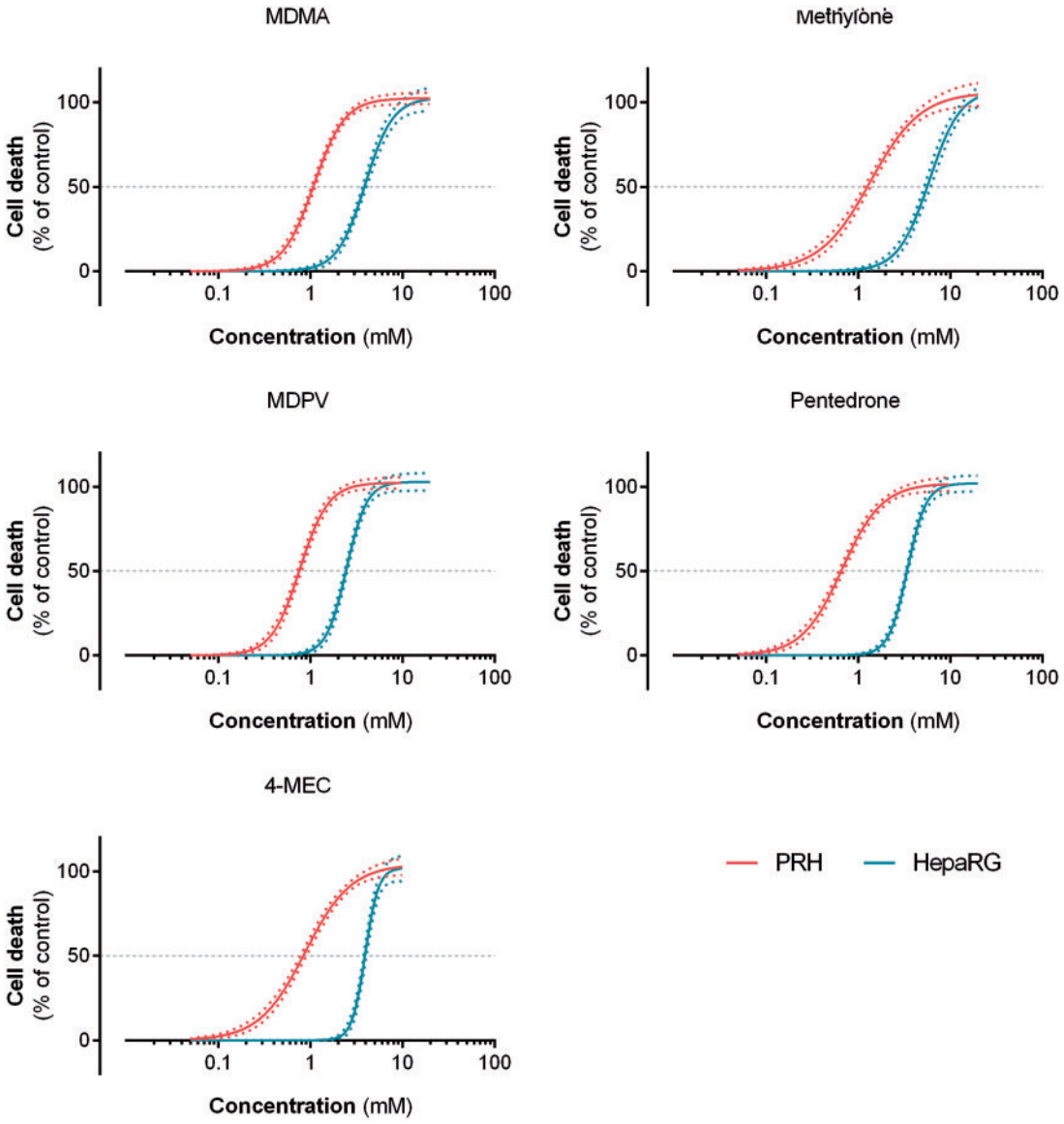

FIG. 1. Nonlinear regression models for the cell death induced by MDMA, methylone, MDPV, pentedrone, and 4-MEC in PRH and HepaRG cells, as evaluated by the MTT reduction assay after 24 h exposure. The mean effects were fitted to the logit function. Dotted lines represent the 95% confidence band of each fit. Results were obtained from at least four independent experiments, performed in triplicate.

As depicted in Table 2, quinidine partially, but significantly, reversed cell death induced by cathinone derivatives in PRH, with a significant increase in MTT reduction for 1.6 mM methylone, MDPV, and pentedrone ($P < .0001$). No significant differences were found between HepaRG cells exposed to the cathinones in the presence or absence of the CYP2D6 inhibitor (data not shown).

Due to the higher sensitivity of PRH to the cytotoxicity elicited by the tested cathinones, all further toxicological evaluations were carried out in this cell model.

Synthetic Cathinones Elicit Hepatotoxicity in Vitro in a concentration-Dependent Manner, with Variable Potency among Derivatives

Exposure of cells to synthetic cathinones resulted in concentration-dependent hepatotoxicity. However, cathinone derivatives displayed different toxic potencies, as follows: pentedrone ≈ MDPV > 4-MEC > methylone. Methylone was the least cytotoxic drug in both cell models, with EC50 values of 1.262 and 5.623 mM in PRH and HepaRG cells, respectively. MDPV and pentedrone were the most toxic compounds in HepaRG cells (EC50 of 2.432 and 3.405 mM) and PRH (EC50 of 0.756 and 0.656 mM, respectively). For both models, these two cathinones were even more hepatotoxic than MDMA (EC50 of 3.854 and 1.070 mM in HepaRG and PRH, respectively; $P < .05$). The toxic potential of 4-MEC was similar to MDMA in HepaRG cells (EC50 of 3.905 mM), but significantly higher in the primary culture (EC50 of 0.835 mM; $P < .01$).

In order to validate MTT reduction data obtained for PRH model, LDH leakage was assessed, as an unbiased test and indicator of cell membrane integrity, under equal experimental conditions. Results obtained from the LDH leakage assay are presented in Figure 2. In accordance to the MTT reduction data, a concentration-dependent increase in extracellular LDH was observed for all compounds. At 1.6 mM, after a 24 h exposure period, MDPV induced an increase on LDH leakage significantly

TABLE 2. Cell viability, as evaluated by the MTT reduction assay after a 24 h exposure of PHR to MDMA, methylone, MDPV, pentedrone and 4-MEC individually (1.6 mM), or in combination with 10 μM quinidine, 1 mM AA, 1mM NAC, or 100 μM Ac-LETD-CHO

Compound	Individual	+ 10 μM quinidine	+ 1 mM AA	+ 1 mM NAC	+ 100 μM Ac-LETD-CHO
MDMA	26.47 ± 1.96	30.79 ± 2.41	39.82 ± 1.51****	33.57 ± 3.06*	34.29 ± 1.26*
Methylone	38.70 ± 1.58	55.44 ± 1.81****	45.33 ± 1.87*	45.76 ± 1.88**	45.70 ± 2.44**
MDPV	4.92 ± 0.45	10.36 ± 0.86****	12.47 ± 1.17****	5.51 ± 0.92	11.85 ± 0.69****
Pentedrone	8.43 ± 0.62	19.46 ± 2.10****	17.77 ± 1.37****	13.44 ± 1.40**	18.86 ± 1.75****
4-MEC	17.72 ± 1.04	20.84 ± 2.46	23.48 ± 1.93*	18.25 ± 1.82	26.92 ± 3.07***

Results are presented as mean ± SEM. *$P < 0.05$; **$P < .01$; ***$P < .001$; ****$P < .0001$ versus individual compounds.

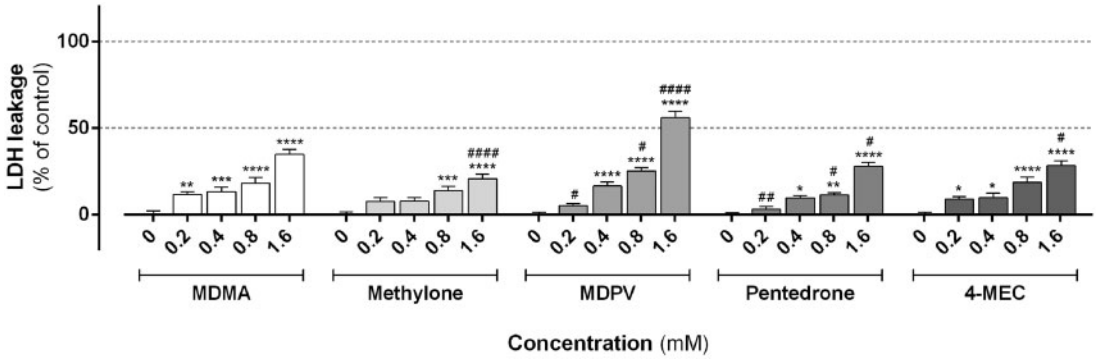

FIG. 2. Extracellular LDH quantification, 24 h after exposure of PHR to MDMA, methylone, MDPV, pentedrone, and 4-MEC. Results were obtained from 6 independent experiments, performed in triplicate. *$P < .05$, ** $P < .01$, *** $P < .001$, **** $P < .0001$ versus control. # $P < .05$, ## $P < .01$, #### $P < .0001$ versus MDMA.

higher than MDMA (56.01 ± 3.61% for MDPV vs. 34.78 ± 2.82% for MDMA, $P < .0001$). At this concentration, 4-MEC, pentedrone and methylone were, in this order, significantly less effective than MDMA (28.35 ± 2.92, 27.86 ± 2.28, and 20.68 ± 2.70%, respectively).

Synthetic Cathinones Have a Strong Reducing Potential

The reducing power assay is often used to evaluate the overall capability of a compound to donate an electron, as compounds with higher reducing power have superior electron-donor ability (Kohen and Nyska, 2002). As depicted in Figure 3, all four cathinones presented a concentration-dependent reducing potential, in the following order of potency: pentedrone ≈4-MEC > methylone > MDPV. To attain a reducing power of 0.5 (Abs = 0.500), the concentrations of cathinones required were 4.161 ± 0.009, 4.230 ± 0.010, 6.047 ± 0.026, and 40.451 ± 0.700 mM for pentedrone, 4-MEC, methylone and MDPV, respectively. MDMA showed an almost negligible reducing power, with an absorbance of 0.042 ± 0.001 for the highest concentration tested, 50 mM.

Synthetic Cathinones Trigger Oxidative Stress in PRH, and Cell Death Is Partially Reversed by Antioxidants

In order to determine the role of oxidative stress in cathinones-induced hepatotoxicity, the formation of ROS and RNS and the intracellular levels of GSH and GSSG were measured in PRH exposed to the cathinone derivatives for 24 h. Our data show that all four cathinone derivatives were capable of stimulating the production of ROS and RNS (Fig. 4). MDMA and MDPV were the least effective compounds, eliciting identical increase of ROS and RNS, only significant at the higher concentration tested (1.23 ± 0.04 and 1.24 ± 0.07 fold increase over control, $P < .0001$). Methylone, 4-MEC and pentedrone induced a significant increase of ROS and RNS production, already observable at a

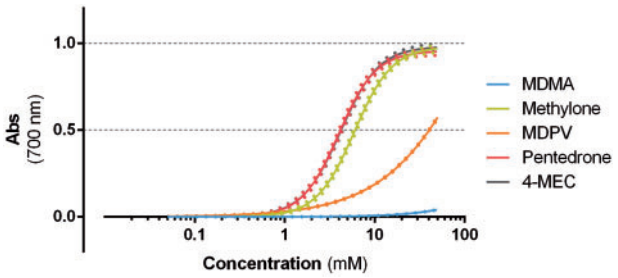

FIG. 3. Nonlinear regression models for the reducing power of MDMA, methylone, MDPV, pentedrone, and 4-MEC. The mean effects were fitted to the logit function. Dotted lines represent the 95% confidence band of each fit. Results were obtained from three independent experiments, performed in duplicate.

concentration as low as 0.4 mM (1.10 ± 0.02, 1.14 ± 0.03, and 1.17 ± 0.02-fold increase over control, respectively, $P < .05$). At 1.6 mM, ROS and RNS production for pentedrone was extensively greater when compared with control (1.56 ± 0.07 fold increase over control, $P < .0001$) and to MDMA at the same concentration. As depicted in Figure 5A, and in accordance to the prior results, pentedrone was also the most effective compound in decreasing the intracellular levels of GSH (23.74 ± 2.19 at 1.6 mM vs. 43.89 ± 4.24 nmol/mg of protein in control cells, $P < .0001$), which is a primary cellular antioxidant. However, the GSH depletion induced by pentedrone was not accompanied by corresponding increases in GSSG levels (Fig. 5B). For the other 4 drugs, a general decrease in GSH levels was followed by an increase in the oxidized form, in an apparent concentration-dependent manner. Nonetheless, no significant differences were observed in the GSH intracellular concentration between any of the synthetic cathinones and MDMA.

To further define the role of oxidative stress in cathinones-induced cell death, two well-described antioxidants were tested in combination with the drugs at 1.6 mM, the concentration at

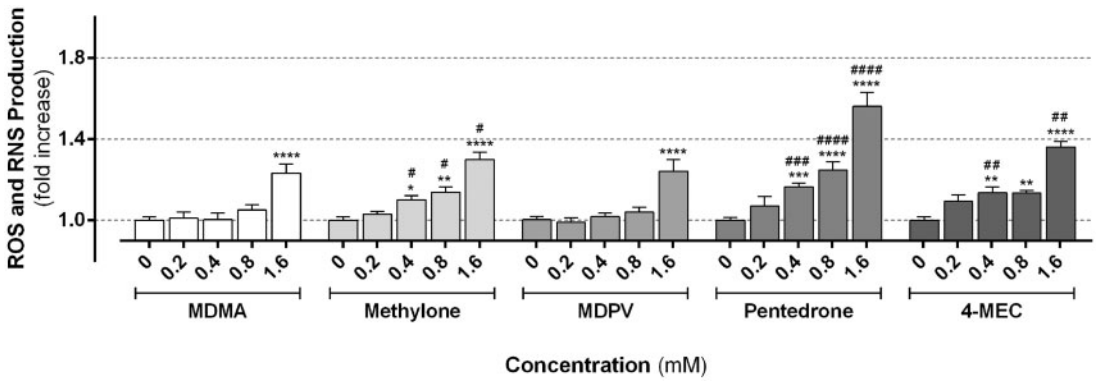

FIG. 4. ROS and RNS production in PHR exposed to MDMA, methylone, MDPV, pentedrone, and 4-MEC, for 24 h. Results were obtained from five independent experiments, performed in triplicate. * $P < .05$, ** $P < .01$, *** $P < .001$, **** $P < .0001$ versus control. # $P < .05$, ## $P < .01$, ### $P < .001$, #### $P < .0001$ versus MDMA.

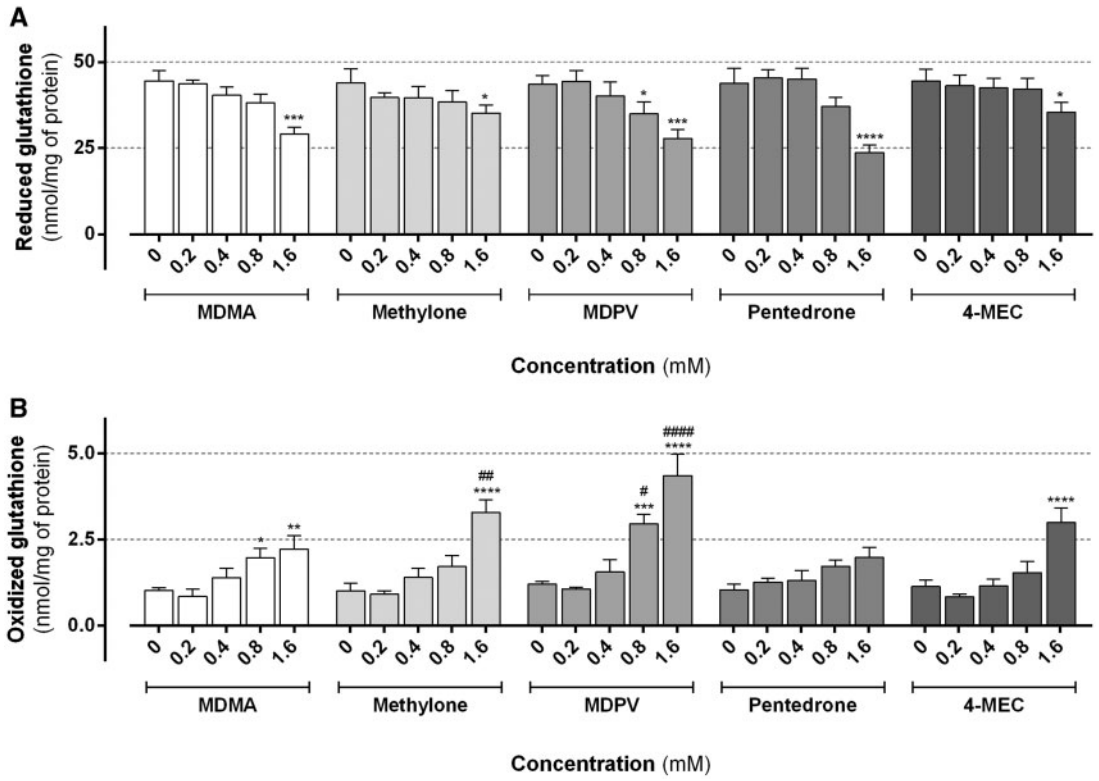

FIG. 5. Intracellular levels of **(A)** GSH and **(B)** GSSG in PHR exposed MDMA, methylone, MDPV, pentedrone and 4-MEC, for 24 h. Results were obtained from five independent experiments, performed in duplicate. * $P < .05$, ** $P < .01$, *** $P < .001$, **** $P < .0001$ versus control. # $P < .05$, ## $P < .01$, #### $P < .0001$ versus MDMA.

which all drugs induce significant increase in ROS and RNS generation and depletion of GSH levels. Results are presented in Table 2. Individually, 1 mM AA and NAC did not show toxicity towards PRH (data not shown). Incubation with AA significantly reversed the cytotoxicity induced by all four synthetic cathinones and MDMA ($P < .05$). This antioxidant effect was more effective with MDMA, pentedrone and MDPV, with a gain of about 13, 9, and 8% in cell viability ($P < .0001$ vs. individual compounds at 1.6 mM), respectively. On the other hand, NAC partially attenuated MDMA, methylone and pentedrone-induced cell death, with a decrease in cell death of about 7% for MDMA and methylone, and 5% for pentedrone ($P < .05$ vs. individual compounds at 1.6 mM). Despite a slight increase in cell viability in PRH exposed to MDPV and 4-MEC in the presence of NAC, this protective effect did not reach statistical significance.

Synthetic Cathinones Disrupt the Hepatocellular Energetic Status

Mitochondria participate in several vital cellular functions, including ATP generation as a source of energy for cells. As depicted in Figure 6, after 24 h of exposure, MDMA, MDPV, and pentedrone were able to significantly reduce ATP intracellular levels at the highest concentration tested, 1.6 mM ($P < .05$). No significant effects were observed with methylone or 4-MEC at any concentrations. MDPV was the most effective drug, inducing a decrease of almost 60% on ATP levels, from 20.65 ± 1.95 in control cells to 8.55 ± 1.67 nmol/mg of protein at 1.6 mM ($P < .001$). At the same concentration, pentedrone and MDMA induced a decline of about 40% of ATP levels. Nonetheless, no significant differences were observed among 1.6 mM

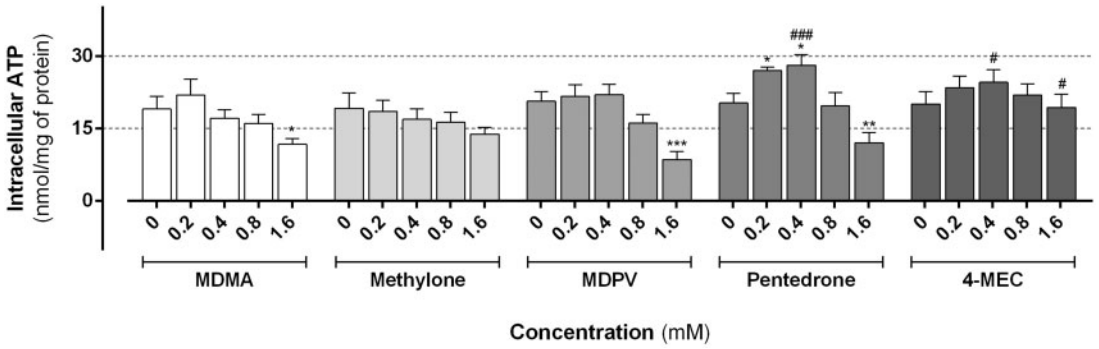

FIG. 6. Intracellular levels of ATP in PHR exposed to MDMA, methylone, MDPV, pentedrone, and 4-MEC, for 24 h. Results were obtained from 5 independent experiments, performed in duplicate. * $P < .05$, ** $P < .01$, *** $P < .001$ versus control. # $P < .05$, #### $P < .0001$ versus MDMA.

pentedrone, MDPV and MDMA. Of note, at lower concentrations (0.2 and 0.4 mM) an increase in ATP production was observed for pentedrone ($P < .05$ vs. control).

Synthetic Cathinones Induce Apoptotic Cell Death, Which Is Partially Reversed by a Caspase Inhibitor

To determine whether synthetic cathinones-induced hepatotoxicity involves programed cell death, the activation of caspase 3 was evaluated as a main event leading to apoptosis. In order to establish the involvement of extrinsic and/or intrinsic pathways, caspases 8 and 9 activities were further analyzed. All four cathinone derivatives induced the activation of the effector caspase, caspase 3, in a concentration-dependent manner (Fig. 7A). For methylone and 4-MEC, this activation was only significant at the higher concentration tested, with an increase of about 60% over control cells ($P < .0001$), but no significant differences were found when compared with MDMA. Although MDMA significantly activated caspase 3 already at 0.4 mM (130.89 ± 11.54%, $P < .05$ vs. control cells), pentedrone and MDPV were the most effective compounds at the higher concentration, with an activation of 254.03 ± 23.45 and 213.60 ± 13.85%, respectively, at 1.6 mM ($P < .0001$ vs. control cells), which was significantly greater than that observed with MDMA at the same concentration (177.51 ± 20.06%, $P < .05$). Similar tendency was observed for caspases 8 and 9 (Figs. 7B and C), with a more pronounced activation with pentedrone and MDPV. At 1.6 mM, these two derivatives led to an activation of 207.80 ± 18.22 and 165.37 ± 5.60% of caspase 8, and 249.14 ± 15.83 and 190.42 ± 7.04% of caspase 9 ($P < .0001$ vs. control cells, $P < .05$ vs. 1.6 mM MDMA). Results are consistent with the activation of both intrinsic (caspase 9) and extrinsic (caspase 8) apoptotic pathways. Thus, the protective potential of Ac-LETD-CHO, a caspase inhibitor known to exert inhibitory effects on caspases 8 and 9, was evaluated. When tested individually, 100 μM Ac-LETD-CHO presented no cytotoxicity (data not shown). The combination of the caspase inhibitor with each compound induced a modest but significant increase of cell viability of about 7–10% when compared with the individual drugs at 1.6 mM ($P < .05$).

The triggering of apoptosis was also demonstrated with Hoechst 33342/PI staining, with evident changes in the chromatin morphology of cells exposed to the synthetic cathinones (Supplementary Figure S1). In control cells, nuclei appear fairly round, with regular contours, and large in size. With the increase in concentration of the drugs, it is evident a reduction of the nuclei size, distinctive of chromatin condensation (eg, 1.6 mM pentedrone compared with control cells), and the presence of pyknotic nuclei, characteristic of early (without PI label, green arrows) and late (with PI label, orange arrows) apoptotic events. In accordance with our data on caspase 3 activation, apoptotic events in MDMA-exposed cells were apparent already at 0.4 mM (Supplementary Figure S1). Nonetheless, a general concentration-dependent increase of apoptotic cells was observed for all compounds, though less evident with methylone. Necrotic cells (large PI-labeled nuclei, red arrows) were more evident at the two highest concentrations tested (0.8 and 1.6 mM).

DISCUSSION

Little is currently known about the potential harms arising from the use of this new generation of cathinone-derived designer drugs. Due to chemical similarity to long-studied amphetamines (particularly MDMA) and the use as alternative for these drugs, similar pharmacodynamics and toxicological mechanisms for β-keto amphetamine-derived designer drugs could be postulated. Thus, there is a great need to study these cathinone derivatives at a fundamental level by comparing their potencies with related amphetamines in order to make risk assessments. In our study, all four synthetic cathinones showed significantly different toxicological potencies in both PRH and HepaRG cells. Methylone was the least cytotoxic substance in both hepatic *in vitro* models, significantly less potent than its non-keto analogue, MDMA, whereas MDPV and pentedrone were more potent than MDMA. 4-MEC was also more toxic than MDMA in PRH, but no significant differences were observed between these two compounds in HepaRG. These results may be partially explained by chemical properties and structures of the compounds in study. Methylone (βk-MDMA) presents a lower log *P* value (1.08) when compared with its related amphetamine MDMA (1.98), which indicates lower lipophilicity as expected from the presence of the β-keto group. On the other hand, the presence of the pyrrolidine ring in cathinones like MDPV greatly reduces their polarity (Coppola and Mondola, 2012), resulting in a greater diffusion of this derivative through cell membranes. In fact, MDPV has the highest log *P* value (2.63) of all cathinones in study, being even higher than MDMA, which is in conformity with the significantly higher increase in toxicity, as evidenced by the LDH leakage assay (Figure 2). Data on extracellular LDH also supports the concentration-dependent pattern observed with the MTT reduction assay. However, the magnitude of loss of integrity of the plasma membrane, as determined by the LDH leakage assay, was lower than the decrease of mitochondrial function, given by the MTT reduction assay. This result was somehow expected since mitochondrial dysfunction often precedes membrane damage, thus explaining the greater sensitivity of the MTT assay.

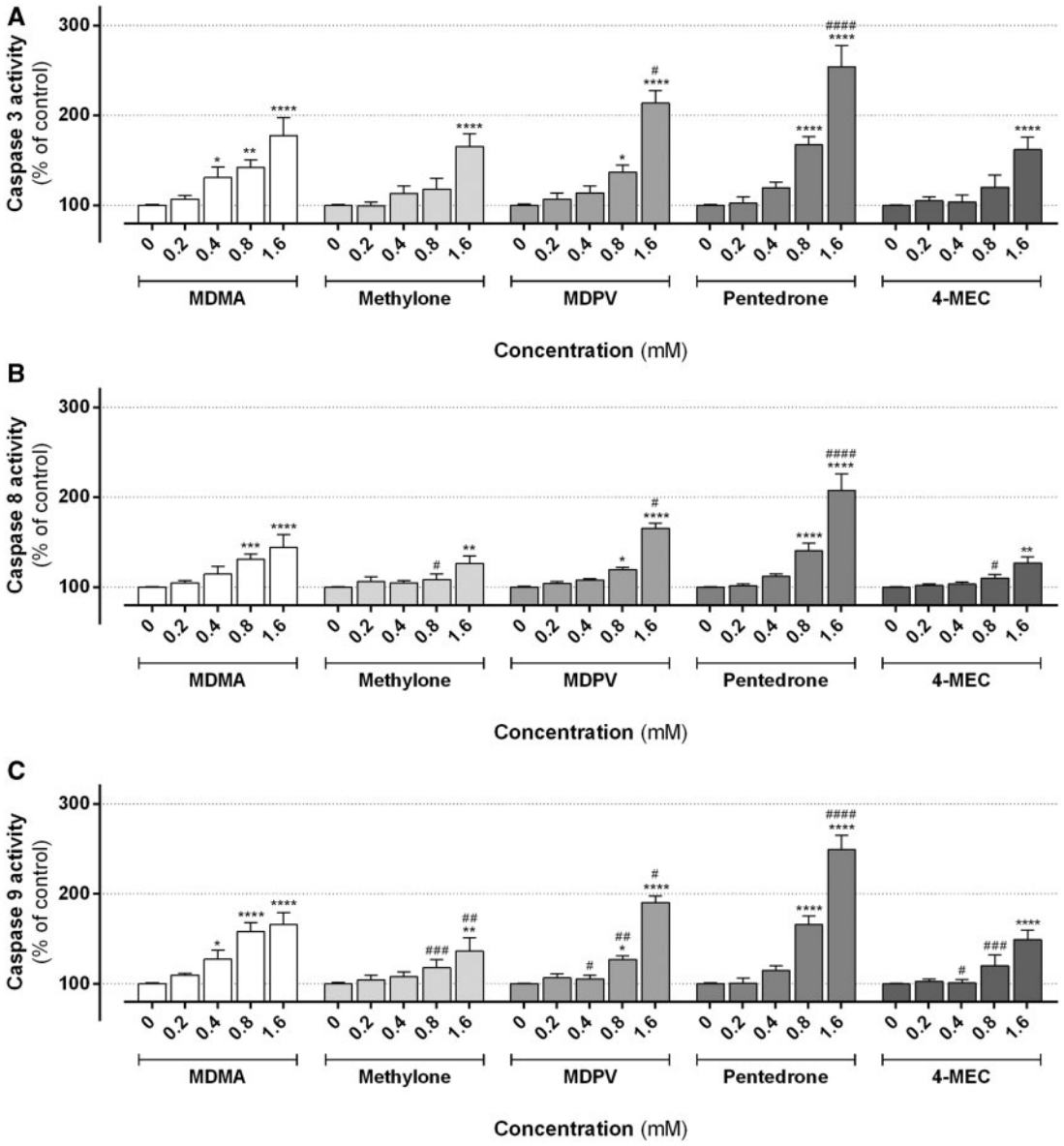

FIG 7. Percentage of increase in caspases **(A)** 3, **(B)** 8, and **(C)** 9 activity in PHR exposed to MDMA, methylone, MDPV, pentedrone and 4-MEC, for 24 h. Results were obtained from four independent experiments, performed in duplicate. * $P < .05$, ** $P < .01$, *** $P < .001$, **** $P < .0001$ versus control. # $P < .05$, ## $P < .01$, ### $P < .001$, #### $P < .0001$ versus MDMA.

The hypothesis of a chemical contribution to the observed cytotoxic effects was further evaluated through the measurement of the redox potential of the cathinone derivatives. As depicted in Figure 3, all four cathinones presented concentration-dependent reducing power. Conversely, MDMA displayed virtually no reducing ability. Accordingly, with a pK_a value of 10.14 (Table 1), MDMA is the stronger base, which means that under physiologic pH (7.4) it is mostly found in the protonated form, and thus detains low electron-donor capacity. When comparing MDMA and its β-keto analogue, the combination of lower pK_a (7.96) and the ability to undergo keto-enol tautomerization (Coppola and Mondola, 2012) may contribute to the higher reducing power of methylone. This is also valid for 4-MEC and pentedrone. On the other hand, despite being the weaker base under study (pK_a value of 7.31), MDPV presents a relatively low reducing potential, which may be a consequence of molecular stabilization by the presence of the pyrrolidine group (Leffler *et al.*, 2014). Our results are in accordance with data from the work of den Hollander *et al.* (2014), which showed significant differences on redox reactivity among several β-keto and non-keto amphetamines, using a tetrazolium redox indicator.

Results show substantial differences between the two cellular models regarding the susceptibility to drug-induced cytotoxicity. HepaRG cells were significantly less sensitive to the toxicity elicited by cathinone derivatives, with EC50 values about 3 to 5 times higher than those observed in PRH (Supplementary Table S1). Under specific culture conditions, the human hepatoma HepaRG cells represent a highly differentiated and metabolically competent liver cell model, capable of expressing both phase I and II drug-metabolizing enzymes as observed *in vivo* (Guillouzo *et al.*, 2007). For this reason, this model has been used as a suitable alternative to human hepatocytes for the study of well-known hepatotoxic compounds (Antherieu *et al.*, 2011; McGill *et al.*, 2011; Sharanek *et al.*, 2014).

However, despite the general advantages of using an immortalized cell line, such as the ease of manipulation, the ability to be cryopreserved and the reduced data variability, the expression of cytochrome P450 enzymes in HepaRG cells is, for most isoenzymes, significantly lower than that observed in freshly isolated human hepatocytes (Aninat *et al.*, 2006), which greatly affects the translation of results into the *in vivo* situation. This is particularly critical for compounds with CYP2D6-dependent metabolism, since this hepatoma cell line was derived from a CYP2D6 poor metabolizer patient (Guillouzo, *et al.*, 2007). In fact, recent evidence suggests that CYP2D6 is the main responsible enzyme for the *in vitro* phase I metabolism of synthetic cathinones (Negreira *et al.*, 2015; Pedersen *et al.*, 2013a, b), which may explain the higher resistance of HepaRG to the synthetic cathinones-induced cytotoxicity. This lower sensitivity of the hepatoma cell line was also observed with MDMA, for which CYP2D6-mediated bioactivation into hepatotoxic metabolites is fully accepted (Carmo *et al.*, 2006; Carvalho *et al.*, 2012). To ascertain whether the CYP2D6 metabolism could explain the higher susceptibility of PRH, both cell models were co-incubated with the cathinones and the CYP2D6 inhibitor, quinidine. A significant reversion in cell death was observed in PRH for methylone, MDPV and pentedrone, while, as expected, no effect was seen in HepaRG cells. Taken together, these findings indicate that PRH is a more suitable *in vitro* model for toxicological studies on synthetic cathinones.

The synthetic cathinones under study triggered oxidative stress as evidenced by enhanced generation of ROS and RNS (Figure 4), and decreases in intracellular GSH levels (Figure 5A). Methylone, 4-MEC and pentedrone were the most potent drugs regarding the formation of ROS and RNS, whereas MDPV and MDMA were only effective at the highest concentration tested. Interestingly, our results show that cathinones-induced ROS and RNS formation appears to be correlated with their reducing potential (electron donor capacity), as derivatives with higher reducing power (methylone, pentedrone, and 4-MEC) elicit greater ROS and RNS production. It is possible that increased reducing power may lead to greater redox cycling of the cathinone metabolites, thereby promoting greater ROS generation, lipid peroxidation, and protein adduction. However, further studies are required to ascertain the contribution of redox properties of the studied drugs to the respective toxicological effects. It is also acknowledged that oxidative stress arises from the disruption of the mitochondrial respiratory chain, contributing to an increase in intracellular ROS and RNS formation (Brookes *et al.*, 2004). Importantly, recent studies have revealed that mephedrone and methylone induce mitochondrial respiratory dysfunction in neuronal cells (den Hollander, *et al.*, 2014, 2015), which is also a recognized mechanism underlying amphetamines-induced toxicity (Carvalho *et al.*, 2012). Furthermore, MDMA is known to undergo extensive hepatic cytochrome P450-mediated bioactivation, with formation of catechols and further oxidation to *o*-quinones, which are highly reactive molecules that may enter redox cycling and lead to the production of ROS and RNS (Carvalho *et al.*, 2010). Since the formation of catechols through *o*-demethylenation was shown to be one of the main metabolic pathways for methylone and MDPV (Pedersen *et al.*, 2013a; Strano-Rossi *et al.*, 2010), it could be anticipated that a similar bioactivation pathway takes place with cathinone derivatives containing the methylenodioxy ring. Nonetheless, further work is needed to elucidate the exact contribution of these mechanisms to the augmented formation of ROS/RNS induced by cathinones.

GSH is a major endogenous antioxidant defense, being responsible for numerous functions while protecting the liver against drug-induced damage (Chen *et al.*, 2013). Since one of these functions is the direct scavenging of superoxide anion and hydroxyl radical, GSH depletion is a foreseeable outcome from the increase in ROS and RNS production. Accordingly, all four cathinones induced a significant decrease in GSH intracellular levels at the higher concentration tested (Figure 5A). Pentedrone was the most effective compound, but no significant increase in GSSG levels was observed after 24 h. The *in vitro* formation of glutathionyl adducts with the demethylenated metabolites of methylenedioxy β-keto amphetamines, including MDPV and methylone, was recently demonstrated (Meyer *et al.*, 2014). However, there is no evidence supporting the ability of cathinones lacking the methylenedioxy ring, such as pentedrone and 4-MEC, to undergo metabolic pathways that result in the formation of conjugates with GSH. For this reason, the absence of a significant increase in GSSG intracellular levels for pentedrone may be due to an ATP-dependent export of the formed GSSG into the extracellular space (Leier *et al.*, 1996). The formation of ROS and RNS and the GSH depletion are well-acknowledged toxicological pathways of MDMA-induced hepatotoxicity (Carvalho *et al.*, 2010), but little is known on the ability of synthetic cathinones to induce oxidative stress. However, some recent studies demonstrated that the cathinone derivative 4-methylmethcathinone (mephedrone) elicits oxidative stress in the brain of rats and mice, characterized by increased lipid peroxidation and altered enzymatic antioxidant systems (Budzynska *et al.*, 2015; Ciudad-Roberts *et al.*, 2016; Lopez-Arnau *et al.*, 2015).

Since oxidative stress appears to underlie the observed hepatotoxicity, it is expected that antioxidants prevent or partially revert the cell death induced by the cathinones. In fact, in our study, 1 mM AA significantly reversed cell death induced by MDMA and all four cathinones, but more pronouncedly for MDMA and its β-keto analogue, while protection with 1 mM NAC was significant only for MDMA, methylone and pentedrone (Table 2). Accordingly, our group has previously demonstrated the protective effects of AA and NAC against the hepatotoxicity elicited by the main MDMA catecholic metabolite, *N*-methyl-α-methyldopamine (Carvalho *et al.*, 2004), as well as the neuroprotection of NAC against the cytotoxicity induced by this metabolite and the GSH conjugate, 5-GSH-α-methyldopamine (Capela *et al.*, 2006). The protective effect of AA is widely acknowledged, and relies on its ability to scavenge ROS and RNS and to regenerate other antioxidants, such as α-tocopherol (Maxwell, 1995). NAC exerts antioxidant effects by acting either directly, as a ROS and RNS scavenger, or indirectly, as a source of cysteine, the precursor for the rate-limiting step of the synthesis of glutathione (Firuzi *et al.*, 2011). This latter function is important when the liver is depleted of GSH, becoming more vulnerable to oxidative damage, which is the case of the synthetic cathinones in this study. Although MDPV is one of the most hepatotoxic compounds, triggering significant depletion of GSH intracellular levels at 1.6 mM, NAC failed to exhibit cytoprotection in the presence of this substance at this concentration. A plausible explanation for these results would be the formation of cytotoxic thioether conjugates of MDPV with NAC and GSH, as it is known to occur with MDMA (Jones *et al.*, 2005), but further studies with MDPV conjugates are required to verify this hypothesis. Since 1.6 mM 4-MEC did not lead to a depletion of GSH or an increase in ROS and RNS production as great as pentedrone, the induction of these oxidative stress pathways may be less preponderant in 4-MEC-induced hepatotoxicity at the conditions tested, thereby explaining the lack of protective effect by NAC.

Used by cells to execute energy-requiring processes, ATP is the primary energy currency, and since mitochondria are the main source of ATP, mitochondrial ATP generation is essential for the maintenance of cellular integrity (Brookes *et al.*, 2004). Our results show that MDPV and pentedrone, as well as MDMA, elicited a significant decline in ATP synthesis after 24 h (Figure 6). This decrease occurred at a concentration where the GSH depletion and the formation of ROS and RNS were significantly increased, especially for pentedrone, suggesting that oxidative stress may be involved in mitochondrial dysfunction. However, despite the decrease in GSH levels observed for methylone and 4-MEC, the mitochondrial damage appears to be insufficient to hamper ATP synthesis with these two derivatives, at least at the range of concentrations tested. The involvement of mitochondria in amphetamines-induced toxicity has been thoroughly reviewed (Barbosa *et al.*, 2015; Carvalho *et al.*, 2012). In response to oxidative injury, the mitochondria undergo extensive changes, including the permeabilization of the mitochondrial membrane, with release of pro-apoptotic proteins into the cytosol, such as cytochrome *c* (Brookes *et al.*, 2004). Once in the cytosol, cytochrome *c* initiates the complex signaling cascade that characterizes the intrinsic mechanisms of apoptosis, with activation of caspase 9 and downstream executioner caspases 3 and 7 that, in turn, cleave intracellular substrates, causing the morphological and biochemical changes that ultimately end in cell death (Tait and Green, 2010; Tsujimoto, 2003). Our data show that all cathinones prompt apoptosis, with activation of both caspases 3 and 9 (Figs. 7A and C). The activation of extrinsic apoptosis was also evaluated through the measurement of caspase 8 activation. This extrinsic pathway is mitochondrion-independent, and it is initiated by the binding of xenobiotics to death receptors located in the surface of cell membrane, with subsequent activation of caspase 8, and further activation of the executioner caspases, or indirect activation of the intrinsic apoptotic pathway (McIlwain *et al.*, 2013). As seen in Figure 7B, all five compounds elicited the activation of caspase 8 in an identical pattern to that observed for caspases 3 and 9. Methylone and 4-MEC were the least effective compounds, which may be expected from the putative inferior potency to induce mitochondrial dysfunction. MDPV and pentedrone, the most hepatotoxic drugs in study, and the most potent compounds concerning ATP depletion and oxidative stress stimulation, respectively, were the most effective triggers of apoptosis, as well. Hoechst 33342/PI staining further supports these findings, with an apparent increase in apoptotic events (green and orange arrows) in a concentration dependent manner (Supplementary Figure S1). This increase was less evident for methylone, which is also the least hepatotoxic drug in study. The presence of necrotic events (red arrows) was also noted at higher concentrations. It is important to note that necrosis is a degradative process that may occur as a primary event of cell death or secondary to apoptosis. Based on our findings showing the absence of necrotic events at lower concentrations of the studied drugs, it seems that the observed LDH release in cells exposed to low concentrations is more likely due to secondary necrosis from late apoptosis. Additionally, the decrease in MTT reduction, a marker of mitochondrial dysfunction, under the same experimental conditions, further supports apoptosis as a main pathway of cell death. For this reason, it was expected that caspase inhibition would detain protective properties against cathinones-induced toxicity. In fact, 100 μM Ac-LETD-CHO, a caspase 8 and 9 inhibitor, significantly reduced the cell death elicited by all cathinones (Table 2). MDPV was previously shown to prompt apoptosis in neonatal mouse brain after acute administration (Adam *et al.*, 2014), whereas the overexpression of the anti-apoptotic Bcl-2 protein partially prevented the cytotoxicity elicited by mephedrone in neuronal cells (den Hollander *et al.*, 2015).

One major limitation of this study is the use of relatively high concentrations of synthetic cathinones when compared with the micromolar levels found in blood samples from 'bath salts'-related intoxications (Gil *et al.*, 2013; Kesha *et al.*, 2013; Pearson *et al.*, 2012; Sykutera *et al.*, 2015). Nonetheless, due to the toxicokinetics, and especially drug distribution and tissue accumulation, it should be noted that the drug concentration to which the liver is actually exposed may be much higher than that found in the blood, to similarly to what was determined for MDMA (Garcıa-Repetto *et al.*, 2003). In fact, it was recently shown that pentedrone and MDPV reach liver-to-blood ratios up to 11 and 23, respectively (Marinetti and Antonides, 2013; Sykutera *et al.*, 2015). Furthermore, it is important to stress that the present work involves a comparative mechanistic study, and the obtained data should be regarded as a means of improving the understanding of the cellular mechanisms that may be involved in the *in vivo* effects of synthetic cathinones.

In conclusion, the present work provided evidence of the hepatotoxicity of cathinone derivatives in *in vitro* models, whose mechanisms may help to understand liver damage reported in humans. Variations in magnitude among the different analogues may be attributable to their chemical properties, including lipophilicity and reducing power, as more lipophilic compounds present greater hepatotoxic potential, and more powerful reducing cathinones elicit enhanced formation of reactive species. Furthermore, this study demonstrated for the first time a common mechanism for cathinones-induced hepatic injury involving oxidative stress and mitochondrial dysfunction. Finally, apoptosis appears to be the main pathway of cell death elicited by these novel drugs, with activation of both intrinsic and extrinsic mechanisms.

SUPPLEMENTARY DATA

Supplementary data are http://toxsci.oxfordjournals.org/

FUNDING

This work was supported by National Funds from Fundação para a Ciência e Tecnologia and Fundo Europeu de Desenvolvimento Regional under Program PT2020 (007265-UID/QUI/50006/2013) and partially from Fundação para a Ciência e Tecnologia funds (UID/Multi/04546/2013). M.J.V. thanks Fundação para a Ciência e Tecnologia for her PhD Grant (SFRH/BD/89879/2012).

REFERENCES

Adam, A., Gerecsei, L. I., Lepesi, N., and Csillag, A. (2014). Apoptotic effects of the 'designer drug' methylenedioxypyrovalerone (MDPV) on the neonatal mouse brain. *Neurotoxicology* **44**, 231–236.

Aninat, C., Piton, A., Glaise, D., Le Charpentier, T.Langouet, S., Morel, F, Guguen-Guillouzo C., and Guillouzo, A., (2006). Expression of cytochromes P450, conjugating enzymes and nuclear receptors in human hepatoma HepaRG cells. *Drug Metab. Dispos.* **34**, 75–83.

Antherieu, S., Rogue, A., Fromenty, B., Guillouzo, A., and Robin, M. A. (2011). Induction of vesicular steatosis by amiodarone and tetracycline is associated with up-regulation of lipogenic genes in HepaRG cells. *Hepatology* **53**, 1895–1905.

Barbosa, D. J., Capela, J. P., Feio-Azevedo, R., Teixeira-Gomes, A., Bastos Mde, L., and Carvalho, F. (2015). Mitochondria: Key players in the neurotoxic effects of amphetamines. *Arch. Toxicol.* **89**, 1695–1725.

Baumann, M. H., Ayestas, M. A., Jr., Partilla, J. S., Sink, J. R., Shulgin, A. T., Daley, P. F., Brandt, S. D., Rothman, R. B., Ruoho, A. E., and Cozzi, N. V. (2012). The designer methcathinone analogs, mephedrone and methylone, are substrates for monoamine transporters in brain tissue. *Neuropsychopharmacology* **37**, 1192–1203.

Baumann, M. H., Partilla, J. S., Lehner, K. R., Thorndike, E. B., Hoffman, A. F., Holy, M., Rothman, R. B., Goldberg, S. R., Lupica, C. R., Sitte, H. H., *et al.* (2013). Powerful cocaine-like actions of 3,4-Methylenedioxypyrovalerone (MDPV), a principal constituent of psychoactive 'bath salts' products. *Neuropsychopharmacology* **38**, 552–562.

Berker, K. I., Guclu, K., Tor, I., and Apak, R. (2007). Comparative evaluation of Fe(III) reducing power-based antioxidant capacity assays in the presence of phenanthroline, bathophenanthroline, tripyridyltriazine (FRAP), and ferricyanide reagents. *Talanta* **72**, 1157–1165.

Borek, H. A., and Holstege, C. P. (2012). Hyperthermia and multiorgan failure after abuse of "bath salts" containing 3,4-methylenedioxypyrovalerone. *Ann. Emerg. Med.* **60**, 103–105, 10.

Brookes, P. S., Yoon, Y., Robotham, J. L., Anders, M. W., and Sheu, S. S. (2004). Calcium, ATP, and ROS: A mitochondrial love-hate triangle. *Am. J. Physiol. Cell Physiol.* **287**, C817–C833.

Budzynska, B., Boguszewska-Czubara, A., Kruk-Slomka, M., Kurzepa, J., and Biala, G. (2015). Mephedrone and nicotine: Oxidative stress and behavioral interactions in animal models. *Neurochem. Res.* **40**, 1083–1093.

Burns, L., Roxburgh, A., Matthews, A., Bruno, R., Lenton, S., and Van Buskirk, J. (2014). The rise of new psychoactive substance use in Australia. *Drug Test. Anal.* **6**, 846–849.

Capela, J. P., Meisel, A., Abreu, A. R., Branco, P. S., Ferreira, L. M., Lobo, A. M., Remiao, F., Bastos, M. L., and Carvalho, F. (2006). Neurotoxicity of Ecstasy metabolites in rat cortical neurons, and influence of hyperthermia. *J. Pharmacol. Exp. Ther.* **316**, 53–61.

Carbone, P. N., Carbone, D. L., Carstairs, S. D., and Luzi, S. A. (2013). Sudden cardiac death associated with methylone use. *Am. J. Forensic Med. Pathol.* **34**, 26–28.

Carmo, H., Brulport, M., Hermes, M., Oesch, F., Silva, R., Ferreira, L. M., Branco, P. S., Boer, D., Remiao, F., Carvalho, F., *et al.* (2006). Influence of CYP2D6 polymorphism on 3,4-methylenedioxymethamphetamine ('Ecstasy') cytotoxicity. *Pharmacogenet. Genomics* **16**, 789-99,

Carvalho, M., Carmo, H., Costa, V. M., Capela, J. P., Pontes, H., Remiao, F., Carvalho, F., and Bastos Mde, L. (2012). Toxicity of amphetamines: An update. *Arch. Toxicol.* **86**, 1167–1231.

Carvalho, M., Pontes, H., Remiao, F., Bastos, M. L., and Carvalho, F. (2010). Mechanisms underlying the hepatotoxic effects of ecstasy. *Curr. Pharm. Biotechnol.* **11**, 476–495.

Carvalho, M., Remiao, F., Milhazes, N., Borges, F., Fernandes, E., Carvalho, F., and Bastos, M. L. (2004). The toxicity of N-methyl-alpha-methyldopamine to freshly isolated rat hepatocytes is prevented by ascorbic acid and N-acetylcysteine. *Toxicology* **200**, 193–203.

Chen, Y., Dong, H., Thompson, D. C., Shertzer, H. G., Nebert, D. W., and Vasiliou, V. (2013). Glutathione defense mechanism in liver injury: Insights from animal models. *Food Chem. Toxicol.* **60**, 38–44.

Ciudad-Roberts, A., Duart-Castells, L., Camarasa, J., Pubill, D., and Escubedo, E. (2016). The combination of ethanol with mephedrone increases the signs of neurotoxicity and impairs neurogenesis and learning in adolescent CD-1 mice. *Toxicol. Appl. Pharmacol.* **293**, 10-20, 10–1016.

Coppola, M., and Mondola, R. (2012). Synthetic cathinones: Chemistry, pharmacology and toxicology of a new class of designer drugs of abuse marketed as "bath salts" or "plant food". *Toxicol. Lett.* **211**, 144–149.

Cozzi, N. V., Sievert, M. K., Shulgin, A. T., Jacob, P, III, and Ruoho, A. E. (1999). Inhibition of plasma membrane monoamine transporters by beta-ketoamphetamines. *Eur. J. Pharmacol.* **381**, 63–69.

DEA, U. S. (2014). National Forensic Laboratory Information System Special Report: Synthetic Cannabinoids and Synthetic Cathinones Reported in NFLIS, 2010–2013. Available at: https://www.nflis.deadiversion.usdoj.gov/. Accessed May 10, 2016.

Deluca, P., Schifano, F., Davey, Z., Corazza, O., Di Furia, L., and Group, P. W. M. R., (2009). MDPV Report. Accessed at http://www.psychonautproject.eu/. Currently unavailable; Accessed May 29, 2013.

den Hollander, B., Sundstrom, M., Pelander, A., Ojanpera, I., Mervaala, E., Korpi, E. R., and Kankuri, E. (2014). Keto amphetamine toxicity-focus on the redox reactivity of the cathinone designer drug mephedrone. *Toxicol. Sci.* **141**, 120–131.

den Hollander, B., Sundstrom, M., Pelander, A., Siltanen, A., Ojanpera, I., Mervaala, E., Korpi, E. R., and Kankuri, E. (2015). Mitochondrial respiratory dysfunction due to the conversion of substituted cathinones to methylbenzamides in SH-SY5Y cells. *Sci. Rep.* **5**, 14924–14910.

Dias da Silva, D., Silva, E., Carvalho, F., and Carmo, H. (2014). Mixtures of 3,4-methylenedioxymethamphetamine (ecstasy) and its major human metabolites act additively to induce significant toxicity to liver cells when combined at low, non-cytotoxic concentrations. *J. Appl. Toxicol.* **34**, 618–627.

Elliott, S., and Evans, J. (2014). A 3-year review of new psychoactive substances in casework. *Forensic Sci. Int.* **243**, 55–60.

EMCDDA (2015a). European Drug Report 2015: Trends and Developments. Available at: http://www.emcdda.europa.eu/. Accessed July 17, 2015.

EMCDDA (2015b). New psychoactive substances in Europe. An update from the EU Early Warning System. Available at: http://www.emcdda.europa.eu/. Accessed July 17, 2015.

Eshleman, A. J., Wolfrum, K. M., Hatfield, M. G., Johnson, R. A., Murphy, K. V., and Janowsky, A. (2013). Substituted methcathinones differ in transporter and receptor interactions. *Biochem. Pharmacol.* **85**, 1803–1815.

Firuzi, O., Miri, R., Tavakkoli, M., and Saso, L. (2011). Antioxidant therapy: Current status and future prospects. *Curr. Med. Chem.* **18**, 3871–3888.

Fröhlich, S., Lambe, E., and O'Dea, J. (2011). Acute liver failure following recreational use of psychotropic "head shop" compounds. *Irish J. Med. Sci.* **180**, 263–264.

Garcıa-Repetto, R., Moreno, E., Soriano, T., Jurado, C., Gimenez, M., and Menendez, M. (2003). Tissue concentrations of MDMA and its metabolite MDA in three fatal cases of overdose. *Forensic Sci. Int.* **135**, 110–114.

Gil, D., Adamowicz, P., Skulska, A., Tokarczyk, B., and Stanaszek, R. (2013). Analysis of 4-MEC in biological and non-biological material–three case reports. *Forensic Sci. Int.* **228**, e11–e15.

Guillouzo, A., Corlu, A., Aninat, C., Glaise, D., Morel, F., and Guguen-Guillouzo, C. (2007). The human hepatoma HepaRG cells: A highly differentiated model for studies of liver metabolism and toxicity of xenobiotics. *Chem. Biol. Int.* **168**, 66–73.

Helander, A., Backberg, M., Hulten, P., Al-Saffar, Y., and Beck, O. (2014). Detection of new psychoactive substance use among emergency room patients: Results from the Swedish STRIDA project. *Forensic Sci. Int.* **243**, 23–29.

Jones, D. C., Duvauchelle, C., Ikegami, A., Olsen, C. M., Lau, S. S., de la Torre, R., and Monks, T. J. (2005). Serotonergic neurotoxic metabolites of ecstasy identified in rat brain. *J. Pharmacol. Exp. Ther.* **313**, 422–431.

Karila, L., Megarbane, B., Cottencin, O., and Lejoyeux, M. (2015). Synthetic cathinones: A new public health problem. *Curr. Neuropharmacol.* **13**, 12–20.

Kelly, J. P. (., and 2011,). Cathinone derivatives: A review of their chemistry, pharmacology and toxicology. *Drug Test. Anal.* **3**, 439–453.

Kesha, K., Boggs, C. L., Ripple, M. G., Allan, C. H., Levine, B., Jufer-Phipps, R., Doyon, S., Chi, P., and Fowler, D. R. (2013). Methylenedioxypyrovalerone ("bath salts"), related death: Case report and review of the literature. *J Forensic Sci.* **58**, 1654–1659.

Kohen, R., and Nyska, A. (2002). Oxidation of biological systems: Oxidative stress phenomena, antioxidants, redox reactions, and methods for their quantification. *Toxicol. Pathol.* **30**, 620–650.

Leffler, A. M., Smith, P. B., de Armas, A., and Dorman, F. L. (2014). The analytical investigation of synthetic street drugs containing cathinone analogs. *Forensic Sci. Int.* **234**, 50–56.

Leier, I., Jedlitschky, G., Buchholz, U., Center, M., Cole, S. P., Deeley, R. G., and Keppler, D. (1996). ATP-dependent glutathione disulphide transport mediated by the MRP gene-encoded conjugate export pump. *Biochem. J.* **314**, 433–437.

Lopez-Arnau, R., Martinez-Clemente, J., Pubill, D., Escubedo, E., and Camarasa, J. (2012). Comparative neuropharmacology of three psychostimulant cathinone derivatives: Butylone, mephedrone and methylone. *Br. J. Pharmacol.* **167**, 407–420.

Lopez-Arnau, R., Martinez-Clemente, J., Rodrigo, T., Pubill, D., Camarasa, J., and Escubedo, E. (2015). Neuronal changes and oxidative stress in adolescent rats after repeated exposure to mephedrone. *Toxicol. Appl. Pharmacol.* **286**, 27–35.

Marinetti, L. J., and Antonides, H. M. (2013). Analysis of synthetic cathinones commonly found in bath salts in human performance and postmortem toxicology: Method development, drug distribution and interpretation of results. *J. Anal. Toxicol.* **37**, 135–146.

Maskell, P. D., De Paoli, G., Seneviratne, C., and Pounder, D. J. (2011). Mephedrone (4-methylmethcathinone)-related deaths. *J. Anal. Toxicol.* **35**, 188–191.

Maxwell, J. C. (2014). Psychoactive substances–some new, some old: A scan of the situation in the U.S. *Drug Alcohol Depend.* **134**, 71–77.

Maxwell, S. R. (1995). Prospects for the use of antioxidant therapies. *Drugs* **49**, 345–361.

McGill, M. R., Yan, H. M., Ramachandran, A., Murray, G. J., Rollins, D. E., and Jaeschke, H. (2011). HepaRG cells: A human model to study mechanisms of acetaminophen hepatotoxicity. *Hepatology* **53**, 974–982.

McIlwain, D. R., Berger, T., and Mak, T. W. (2013). Caspase functions in cell death and disease. *Cold Spring Harbor Perspectives in Biology* **5**, a008656.

Meyer, M. R., Richter, L. H., and Maurer, H. H. (2014). Methylenedioxy designer drugs: Mass spectrometric characterization of their glutathione conjugates by means of liquid chromatography-high-resolution mass spectrometry/mass spectrometry and studies on their glutathionyl transferase inhibition potency. *Anal. Chim. Acta* **822**, 37–50.

Moran, J., and Seely, K. (2014). Bath salts: Understanding a pervasive designer drug. *Clin. Lab. News* 1–4.

Murray, B. L., Murphy, C. M., and Beuhler, M. C. (2012). Death following recreational use of designer drug "bath salts" containing 3,4-Methylenedioxypyrovalerone (MDPV). *J. Med. Toxicol.* **8**, 69–75.

Negreira, N., Erratico, C., Kosjek, T., van Nuijs, A. L., Heath, E., Neels, H., and Covaci, A. (2015). In vitro Phase I and Phase II metabolism of alpha-pyrrolidinovalerophenone (alpha-PVP), methylenedioxypyrovalerone (MDPV) and methedrone by human liver microsomes and human liver cytosol. *Anal. Bioanal. Chem.* **407**, 5803–5816.

Pearson, J. M., Hargraves, T. L., Hair, L. S., Massucci, C. J., Frazee, C. C.III., and Garg, U Pietak, B. R. (2012). Three fatal intoxications due to methylone. *J. Anal. Toxicol.* **36**, 444–451.

Pedersen, A. J., Petersen, T. H., and Linnet, K. (2013a). In vitro metabolism and pharmacokinetic studies on methylone. *Drug Metab. Dispos.* **41**, 1247–1255.

Pedersen, A. J., Reitzel, L. A., Johansen, S. S., and Linnet, K. (2013b). In vitro metabolism studies on mephedrone and analysis of forensic cases. *Drug Test. Anal.* **5**, 430–438.

Prosser, J. M., and NelsonL. S. (2012). The toxicology of bath salts: A review of synthetic cathinones. *J. Med. Toxicol.***8**, 33–42.

Regunath, H., Ariyamuthu, V. K., Dalal, P., and Misra, M. (2012). Bath salt intoxication causing acute kidney injury requiring hemodialysis. *Hemodial. Int.* **16(Suppl 1)**, S47–S49.

Ross, E. A., Watson, M., and Goldberger, B. (2011). "Bath salts" intoxication. *N. Engl. J. Med.* **365**, 967–968.

Sharanek, A., Azzi, P. B., Al-Attrache, H., Savary, C. C., Humbert, L., Rainteau, D., Guguen-Guillouzo, C., and Guillouzo, A. (2014). Different dose-dependent mechanisms are involved in early cyclosporine a-induced cholestatic effects in hepaRG cells. *Toxicol. Sci.* **141**, 244–253.

Simmler, L. D., Buser, T. A., Donzelli, M., Schramm, Y., Dieu, L. H., Huwyler, J., Chaboz, S., Hoener, M. C., and Liechti, M. E. (2013). Pharmacological characterization of designer cathinones in vitro. *Br. J. Pharmacol.* **168**, 458–470.

Simmler, L. D., Rickli, A., Hoener, M. C., and Liechti, M. E. (2014). Monoamine transporter and receptor interaction profiles of a new series of designer cathinones. *Neuropharmacology* **79**, 152–160.

Sitte, H. H., and Freissmuth, M. (2010). The reverse operation of Na(+)/Cl(-)-coupled neurotransmitter transporters–why amphetamines take two to tango. *J. Neurochem.* **112**, 340–355.

Strano-Rossi, S., Cadwallader, A. B., de la Torre, X., and Botre, F. (2010). Toxicological determination and in vitro metabolism of the designer drug methylenedioxypyrovalerone (MDPV) by gas chromatography/mass spectrometry and liquid chromatography/quadrupole time-of-flight mass spectrometry. *Rapid Commun. Mass Spectrom.* **24**, 2706–2714.

Sykutera, M., Cychowska, M., and Bloch-Boguslawska, E. (2015). A fatal case of pentedrone and alpha-pyrrolidinovalerophenone poisoning. *J. Anal. Toxicol.gy* **39**, 324–329.

Tait, S. W., and Green, D. R. (2010). Mitochondria and cell death: Outer membrane permeabilization and beyond. *Nat. Rev. Mol. Cell Biol.* **11**, 621–632.

Tsujimoto, Y. (2003). Cell death regulation by the Bcl-2 protein family in the mitochondria. *J. Cell. Physiol.* **195**, 158–167.

Valente, M. J., Araujo, A. M., Silva, R., Bastos, M. L., Carvalho, F., Guedes de Pinho, P., and Carvalho, M. 3,4-Methylenedioxypyrovalerone (MDPV): In vitro mechanisms of hepatotoxicity under normothermic and hyperthermic conditions. *Arch. Toxicol.* Forthcoming.

Valente, M. J., Guedes de Pinho, P., de Lourdes Bastos, M., Carvalho, F., and Carvalho, M. (2014). Khat and synthetic cathinones: A review. *Arch. Toxicol.* **88**, 15–45.

Van Hout, M. C. (2014). An internet study of user's experiences of the synthetic cathinone 4-methylethcathinone (4-MEC). *J. Psychoactive Drugs* **46**, 273–286.

Westphal, F., Junge, T., Rosner, P., Fritschi, G., Klein, B., and Girreser, U. (2007). Mass spectral and NMR spectral data of two new designer drugs with an alpha-aminophenone structure: 4'-methyl-alpha-pyrrolidinohexanophenone and 4'-methyl-alpha-pyrrolidinobutyrophenone. *Forensic Sci. Int.* **169**, 32–42.

Available at: www.drugs-forum.com. Accessed September 28, 2015.